Materials science / Материаловедение

UDC 536.425:539.25:539.351
DOI 10.17073/0368-0797-2023-5-587-593

Original article
Оригинальная статья

Formation of the gradient of structural-phase states of high-speed steel during surfacing. Part 1. Solving the Stefan problem with two movable boundaries

S. A. Nevskii[1], L. P. Bashchenko[1], O. A. Peregudov[2]

[1] **Siberian State Industrial University** (42 Kirova Str., Novokuznetsk, Kemerovo Region – Kuzbass 654007, Russian Federation)
[2] **Omsk State Technical University** (11 Mira Ave., Omsk 644050, Russian Federation)

nevskiy.sergei@yandex.ru

Abstract. The article considers theoretical study of solidification of the binary iron–tungsten system at a tungsten content of 18 wt. %. Such tungsten content is typical for heat-resistant alloys used in plasma-arc surfacing on the rolls surface. The axisymmetric Stefan thermal problem is solved for two movable cylindrical boundaries that separate three regions. In region *1*, the melt is at the melting point; in region *2*, the substance is in a two–phase state, and in region *3* – a solid. The liquidus temperature was set at the interface of regions *1* and *2*, and the solidus temperature – at the interface of regions *2* and *3*. At these boundaries, a condition for the heat flows balance was given, from which a system of kinetic equations was obtained. This system was solved by numerical methods, without hypothesizing that the fronts of phase transformations move according to the law $R \sim t^{1/2}$. Solution of the system of kinetic equations shows that the solidus boundary moves almost linearly. The liquidus boundary moves according to the parabolic law. For regions of the micrometer range in size, the processes of phase transformations take place in a time of about 5 ns, whereas for regions of the order of 10 μm in size – in a time of about 50 ms. Dependences of temperature fields on the radial coordinate at various points in time show that with increasing time, the dimensions of region *2* decrease, and as soon as coordinates of the liquidus and solidus boundaries become close, thecrystallization process stops. Further development of the model consists in taking into account the rotation of one of the media. The results obtained will serve as a material for the study of the Mullins-Sekerka two-front instability.

Keywords: iron – tungsten system, the Stefan problem, equation of thermal conductivity, moving boundaries of phase transformations

Acknowledgements: The research was supported by the Russian Science Foundation (grant No. 23-19-00186, https://rscf.ru/project/23-19-00186).

For citation: Nevskii S.A., Bashchenko L.P., Peregudov O.A. Formation of the gradient of structural-phase states of high-speed steel during surfacing. Part 1. Solving the Stefan problem with two movable boundaries. *Izvestiya. Ferrous Metallurgy*. 2023;66(5):587–593.
https://doi.org/10.17073/0368-0797-2023-5-587-593

Формирование градиента структурно-фазовых состояний быстрорежущей стали при наплавке. Часть 1. Решение задачи Стефана с двумя подвижными границами

С. А. Невский[1], Л. П. Бащенко[1], О. А. Перегудов[2]

[1] **Сибирский государственный индустриальный университет** (Россия, 654007, Кемеровская обл. – Кузбасс, Новокузнецк, ул. Кирова, 42)
[2] **Омский государственный технический университет** (Россия, 644050, Омск, пр. Мира, 11)

nevskiy.sergei@yandex.ru

Аннотация. Теоретически рассматривается процесс затвердевания бинарной системы железо – вольфрам при содержании вольфрама 18 % (по массе). Такое содержание вольфрама характерно для теплостойкого сплава, который применяется в процессах плазменно-дуговой наплавки на поверхность валков. Решается осесимметричная тепловая задача Стефана для двух подвижных цилиндрических границ, которые разделяют три области. В области *1* расплав находится при температуре плавления, в области *2* вещество находится в двухфазном состоянии, а в области *3* – твердое тело. На границе раздела областей *1* и *2* задается температура ликвидуса, а на границе раздела *2* и *3* –

температура солидуса. На данных границах задается условие баланса тепловых потоков, из которого получена система кинетических уравнений. Эту систему решали численными методами, при этом не выдвигались гипотезы о том, что фронты фазовых превращений движутся по закону $R \sim t^{1/2}$. Решение системы кинетических уравнений показывает, что граница солидуса движется практически по линейному закону. Граница ликвидуса перемещается по параболическому закону. Для областей микрометрового диапазона по размерам процессы фазовых превращений протекают за время порядка 5 нс, тогда как для областей размерами порядка 10 мкм – за время около 50 мкс. Зависимости температурных полей от радиальной координаты в различные моменты времени показывают, что с увеличением времени размеры области *2* уменьшаются, и, как только значения координат границ ликвидуса и солидуса становятся близкими, процесс кристаллизации останавливается. Дальнейшее развитие модели заключается в учете вращения одной из сред. Полученные результаты послужат материалом для исследования двухфронтовой неустойчивости Маллинза-Секерки.

Ключевые слова: система железо – вольфрам, задача Стефана, уравнение теплопроводности, подвижные границы фазовых превращений

Благодарности: Исследование выполнено при финансовой поддержке Российского научного фонда (грант № 23-19-00186), https://rscf.ru/project/23-19-00186).

Для цитирования: Невский С.А., Бащенко Л.П., Перегудов О.А. Формирование градиента структурно-фазовых состояний быстрорежущей стали при наплавке. Часть 1. Решение задачи Стефана с двумя подвижными границами. *Известия вузов. Черная металлургия*. 2023;66(5):587–593. *https://doi.org/10.17073/0368-0797-2023-5-587-593*

Introduction

The methods involving plasma surfacing of different wear-resistant materials are commonly employed for the restoration or repair of forming rolls [1]. Among the surfacing materials, there is a specific interest in heat-resistant iron-based alloys with elevated tungsten levels (approximately 17 – 18 %) and carbon content (0.76 – 0.82 %), renowned for their high hardness and exceptional wear resistance [2]. To prevent the formation of cold cracks during the application of coatings made from such alloys, pre-heating and controlled slow cooling of the parts are utilized [3]. However, post this treatment, the coatings exhibit reduced hardness and wear resistance. A complex heat treatment process (involving annealing, hardening, and tempering) becomes necessary to enhance these properties. Yet, this significantly restricts the potential applications of these considered alloys [4]. Hence, finding plasma surfacing methods for heat-resistant alloys that circumvent crack formation while preserving high mechanical and tribological properties without the need for additional thermal treatments is crucial. Addressing this challenge requires an understanding of the mechanisms governing the formation of gradient structural-phase states in materials during surfacing. The crystallization processes of the materials play a pivotal role in shaping these states [5], ultimately determining the resulting structure and hence, the mechanical properties achieved during the surfacing process.

Currently, numerous papers [5 – 10] expound upon mechanisms and models pertaining to the crystallization of materials on surfaces of various geometries. Depending on the external factors such as cooling rate, rotation speed, ambient temperature, degree of supercooling, among others, the resulting structure can manifest as cellular, dendritic, or a combination of both structures concurrently [5; 6]. One of the main mechanisms driving their formation, as proposed in [7; 8], involves the instability of the crystallization front induced by the temperature decrease during the phase transition, caused by the expulsion of impurities into the melt and the phenomenon of solutal undercooling. Hence, the configuration of the interfacial boundary significantly influences the impurity distribution within the crystal [9]. The central consensus across all theories of morphological stability is that when a specific balance between temperature and concentration gradients is reached, the crystallization front becomes unstable to minor perturbations [10]. Consequently, intricate structural-phase states emerge, facilitating particle nucleation on dissolved impurities. This leads to the creation of an extended phase transition region preceding the crystallization front [11]. Notably, the models outlined in [5 – 11] solely consider the displacement of phase transition boundaries, disregarding the displacement of melt heating boundaries. Typically, it is assumed that this boundary either maintains a stabilized temperature distribution or extends infinitely [12; 13]. Recognizing the outcomes of resolving the thermal problem, where the heating boundary is not considered infinitely large [14], reveals that the growth rate of particles accelerates in comparison to scenarios where this aspect is disregarded. Consequently, in the development of mathematical models concerning the impact of plasma on material structure, it becomes imperative to consider not only the displacement of phase transition boundaries but also the shifting boundaries of heating. In the quest to understand the mechanisms governing the formation of gradient structures and phase compositions in heat-resistant alloys during plasma surfacing on rotating rolls, integrating the concepts associated with the emergence and progression of the Mullins–Sekerka instability [15] becomes crucial. Analyzing this instability aids in determining the conditions for the onset of these states, taking into consideration the shifts in the heating boundary. This instability is studied through several stages: initially determining the nature of interface perturbations and evaluating the impact of its curvature on the liquidus temperature. Subsequently, calculations are performed for the temperature and concentration fields within

the solid and liquid phases. This analysis includes identifying the dependency of the perturbation growth rate on the conditions existing at the phase transition boundary.

The focal point of this paper revolves around resolving the thermal and diffusion Stefan problem involving two movable boundaries. This approach facilitates the monitoring of material solidification kinetics. Unlike conventional studies [16 – 18] that rely on the assumption of crystal growth being directly proportional to $t^{1/2}$ this hypothesis is deliberately avoided in this investigation. Instead, the evolution of crystal growth over time is tracked by solving a system of kinetic equations derived from temperature and substance balance conditions at the phase transition boundaries.

Research methodology (setting up a problem)

Let us examine the process of directional solidification along the spatial axis r in a cylindrical front. Fig. 1 illustrates the geometry of the problem.

The initial phase occupies the region $R_2(t) < r < +\infty$ (where t represents time) and maintains a temperature of T_0. When the temperature T^{**} is attained, the second phase forms, which occupies the region $R_1(t) < r < R_2(t)$. At temperature T^*, the third phase emerges within the region $0 < r < R_1(t)$. Let us formulate the thermal conductivity equation for each of these distinct regions:

$$\begin{aligned}
&\frac{\partial T_1}{\partial t} = \chi_1\left[\frac{1}{r}\frac{\partial}{\partial r}\left(r\frac{\partial T_1}{\partial r}\right)\right],\ R_2(t) < r < +\infty;\\
&\frac{\partial T_2}{\partial t} = \chi_2\left[\frac{1}{r}\frac{\partial}{\partial r}\left(r\frac{\partial T_2}{\partial r}\right)\right],\ R_1(t) < r < R_2(t);\\
&\frac{\partial T_3}{\partial t} = \chi_3\left[\frac{1}{r}\frac{\partial}{\partial r}\left(r\frac{\partial T_3}{\partial r}\right)\right],\ 0 < r < R_1(t),
\end{aligned} \tag{1}$$

where χ_1 and χ_2, χ_3 are thermal diffusivity coefficients in regions *1 – 3*.

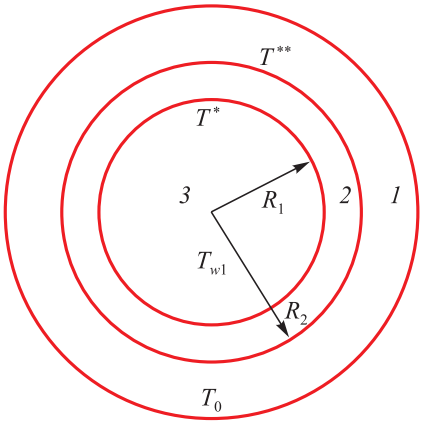

Fig. 1. Diagram of the problem geometry

Рис. 1. Схема геометрии задачи

The shift in phase transition boundaries is determined based on the balance conditions of temperature and heat flows, as expressed by equations (2):

$$\begin{aligned}
&T_3 = T_2 = T^*,\ r = R_1(t);\\
&-\lambda_3\frac{\partial T_3}{\partial r} + \lambda_2\frac{\partial T_2}{\partial r} = \Delta H_1\frac{dR_1}{dt},\ r = R_1(t);\\
&T_2 = T_1 = T^{**},\ r = R_2(t);\\
&\lambda_1\frac{\partial T_1}{\partial r} - \lambda_2\frac{\partial T_2}{\partial r} = \Delta H_2\frac{dR_2}{dt},\ r = R_2(t),
\end{aligned} \tag{2}$$

where λ_1 and λ_2, λ_3 are thermal conductivity coefficients in the regions *1 – 3*; ΔH_1 and ΔH_2 represent the volumetric heat of phase transformations.

At $r \to 0$, the temperature is T_{w1}, and at $r \to \infty$, the temperature is T_0. The initial conditions are defined as

$$T_2(r,\ 0) = T_0;\ R_1(0) = R_0;\ R_2(0) = R_0^*, \tag{3}$$

where R_0 and R_0^* are the initial radii of the phase transition boundaries.

The solution of this system of equations (1) – (3) is determined as follows

$$T_i(r,\ t) = A_i + B_i E_i\left(\frac{r^2}{4\chi_i t}\right), \tag{4}$$

where A_i, B_i are arbitrary constants; $E_i(z)$ is an integral exponent; $i = 1 \div 3$.

Applying the boundary conditions (2) and initial conditions (3) to formula (4), the resulting solution is as follows:

$$\begin{aligned}
&T_1(r,\ t) = T_0 - \left(T_0 - T^{**}\right)\frac{E_i\left(\frac{r^2}{4\chi_1 t}\right)}{E_i\left(\frac{R_2^2}{4\chi_1 t}\right)},\\
&R_2(t) < r < +\infty;\\
&T_2(r,\ t) = \left[T^{**}E_i\left(\frac{R_1^2}{4\chi_2 t}\right) - T^*E_i\left(\frac{R_2^2}{4\chi_2 t}\right) + \left(T^* - T^{**}\right)\times\right.\\
&\left.\times E_i\left(\frac{r^2}{4\chi_2 t}\right)\right]\Big/\left[E_i\left(\frac{R_1}{4\chi_2 t}\right) - E_i\left(\frac{R_2}{4\chi_2 t}\right)\right],\\
&R_1(t) < r < R_2(t);\\
&T_3(r,\ t) = \left[T^*E_i\left(\frac{R^2}{4\chi_3 t}\right) - T_{w1}E_i\left(\frac{R_1^2}{4\chi_3 t}\right) - \left(T^* - T_{w1}\right)\times\right.\\
&\left.\times E_i\left(\frac{r^2}{4\chi_3 t}\right)\right]\Big/\left[E_i\left(\frac{R^2}{4\chi_3 t}\right) - E_i\left(\frac{R_1^2}{4\chi_3 t}\right)\right],\\
&0 < r < R_1(t).
\end{aligned} \tag{5}$$

The parameter R, introduced to prevent divergence at $r \to 0$, is assigned a value of 10^{-8} m to eliminate the singularity at this point in the radial coordinate.

Results and discussion

As equation (5) is integrated into the heat balance equations at the boundaries of phase transitions, the resulting kinetic equations are as follows:

$$\frac{dR_1}{dt} = \frac{\left[F_1 \exp\left(-\frac{R_1^2}{4\chi_1 t}\right)\right] - \left[F_2 \exp\left(-\frac{R_1^2}{4\chi_3 t}\right)\right]}{R_1\left[E_i\left(\frac{R_1^2}{4\chi_2 t}\right) - E_i\left(\frac{R_2^2}{4\chi_2 t}\right)\right]};$$

$$\frac{dR_2}{dt} = \frac{G_1 \exp\left(-\frac{R_2^2}{4\chi_2 t}\right)}{R_2\left[E_i\left(\frac{R_1^2}{4\chi_2 t}\right) - E_i\left(\frac{R_2^2}{4\chi_2 t}\right)\right]} - \frac{G_2 \exp\left(-\frac{R_2^2}{4\chi_1 t}\right)}{R_2\left[E_i\left(\frac{R_2^2}{4\chi_1 t}\right)\right]}; \quad (6)$$

$$F_1 = \frac{2\left(T^{**} - T^*\right)\lambda_2}{\Delta H_1}; \; F_2 = \frac{2\left(T^* - T_{w1}\right)\lambda_3}{\Delta H_1};$$

$$G_1 = \frac{2\left(T^* - T^{**}\right)\lambda_2}{\Delta H_2}; \; G_2 = \frac{2\left(T_0 - T^{**}\right)\lambda_1}{\Delta H_2}.$$

The system (6) of ordinary differential equations is resolved using the high-order Runge-Kutta method. To simplify the mathematical computations, non-dimensional variables $\tilde{R}_i = \frac{R}{R_0}$ and $\tau = t\frac{\chi_1}{R_0^2}$ (where τ is nondimensional time) were employed. Given that as at $t \to 0$, the function $E_i \frac{R_i^2}{4\chi t} \to 0$, the initial time value was set to 10^{-9} s. The characteristics of the investigated material, specifically, iron – tungsten system, are outlined in the table provided.

Characteristics of the iron – tungsten system

Характеристики системы железо – вольфрам

Material characteristics	Designation	Value
Melt temperature, K	T_{w1}	1811
Specific heat of fusion, kJ/kg	ΔH	270
Density, kg/m^3	ρ_1	6980
Thermal conductivity of material, W/(m·K)		
in region *1*	λ_1	39
in region *2*	λ_2	35
in region *3*	λ_3	35
Thermal diffusivity of material, m^2/s		
in region *1*	χ_1	$6.8 \cdot 10^{-6}$
in region *2*	χ_2	$6.9 \cdot 10^{-6}$
in region *3*	χ_3	$6.9 \cdot 10^{-6}$

In region *1*, the initial melt temperature was set at $T_0 = 1811$ K. At the R_2 boundary, the liquidus temperature T^{**} is 1806 K, while at the R_1 boundary, the solidus temperature T^* is 1803 K. These temperatures were determined based on the state diagram [19] for an 18 wt. % tungsten content. The temperature T_{w1} was assumed to be lower than T^* and measured at 1790 K. It was considered that $\chi_2 = \chi_3$ and $\lambda_2 = \lambda_3$, along with $\Delta H_1 = \Delta H_2$. Fig. 2 displays the dependencies of the interface movements. At $R_0 = 1$ μm, the boundary coordinate R_1 exhibits nearly linear growth until $\tau = 0.028$ (4.4118 ns), while R_2 demonstrates non-monotonic changes, decreasing after $\tau > 0.028$ (4.4118 ns). For $R_0 = 10$ μm, a similar trend is observed yet the crystallization process takes place over a longer duration of 41.176 μs.

The results suggest that with a reduction in the size of nuclei, the duration of their steady growth significantly decreases by almost four orders of magnitude. The abrupt decline in the radial coordinate R_2 may indicate instability in the crystallization front, potentially due to interfacial surface tension and supercooling effects. The rapidity of the crystallization process in smaller regions is attributed to a high surface energy, which aims to decrease through size growth and interface configuration changes. In Fig. 3, the temperature dependencies plotted against the non-dimensional radial coordinate illustrate a notable trend: as time progresses, region *2* demonstrates a reduction in size (represented by curves *2* and *3*), while conversely, region *3*, displays growth.

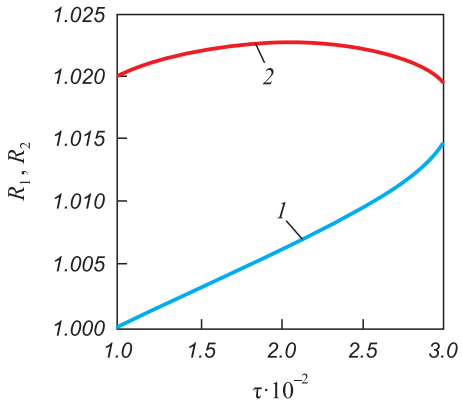

Fig. 2. Dependences of radial coordinates of crystallization front on time at $T_{w1} = 1790$ K, $T^* = 1803$ K, $T^{**} = 1806$ K, $T_0 = 1811$ K, $R_0 = 1$ μm:
1 – boundary of transition between phases *1* and *2*;
2 – boundary of transition between phases *2* and *3*

Рис. 2. Зависимости радиальных координат фронта кристаллизации от времени при $T_{w1} = 1790$ K, $T^* = 1803$ K, $T^{**} = 1806$ K, $T_0 = 1811$ K, $R_0 = 1$ мкм:
1 – граница перехода между фазами *1* и *2*;
2 – граница перехода между фазами *2* и *3*

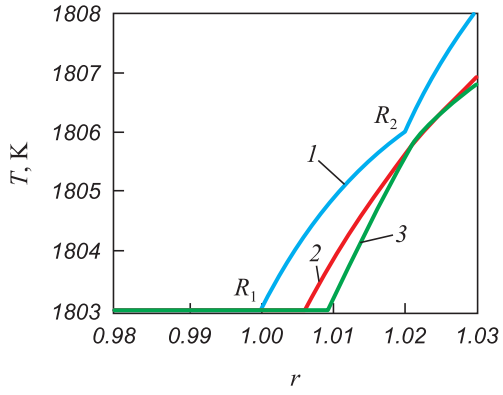

Fig. 3. Temperature dependences on the coordinate at different time points at T_{w1} = 1790 K, T^* = 1803 K, T^{**} = 1806 K, T_0 = 1811 K, R_0 = 1 μm: *1* – τ = 0.01; *2* – τ = 0.02; *3* – τ = 0.025

Рис. 3. Зависимости температуры от координаты в различные моменты времени при T_{w1} = 1790 K, T^* = 1803 K, T^{**} = 1806 K, T_0 = 1811 K, R_0 = 1 мкм: *1* – τ = 0,01; *2* – τ = 0,02; *3* – τ = 0,025

In the scenario where T_0 = 1790 K, T^{**} = 1803 K, T^* = 1803 K and T_{w1} = 1811 K (Fig. 4). The coordinates of the phase transition boundaries exhibit a reduction (Fig. 4, *a*), with R_1 decreasing linearly while R_2 follows a parabolic trajectory. Temperature dependences (Fig. 4, *b*) indicate a similar trend to the previous case, wherein regions *2* and *3* (curves *2* and *3*) experience a decrease in size.

Conclusions

The theoretical investigation of the crystallization process within the iron – tungsten system, conducted by solving kinetic equations, revealed intriguing behavior. Specifically, it was observed that the movement of the liquidus boundary R_2 follows a descending parabolic trajectory, contrary to the expected $R \sim t^{1/2}$ law, whereas the solidus boundary R_1 exhibits almost linear movement. Upon reaching a certain time threshold, the convergence of these boundaries occurs, indicating either the cessation of the crystallization process or the onset of crystallization front instability. The temperature dependencies derived from this study will serve as a foundational framework for further exploration of this observed instability. As the model progresses and adapts to simulate the plasma-arc surfacing process of rolls, future iterations will consider factors such as the rotation of one of the media involved and a more precise incorporation of the concentration of alloying elements.

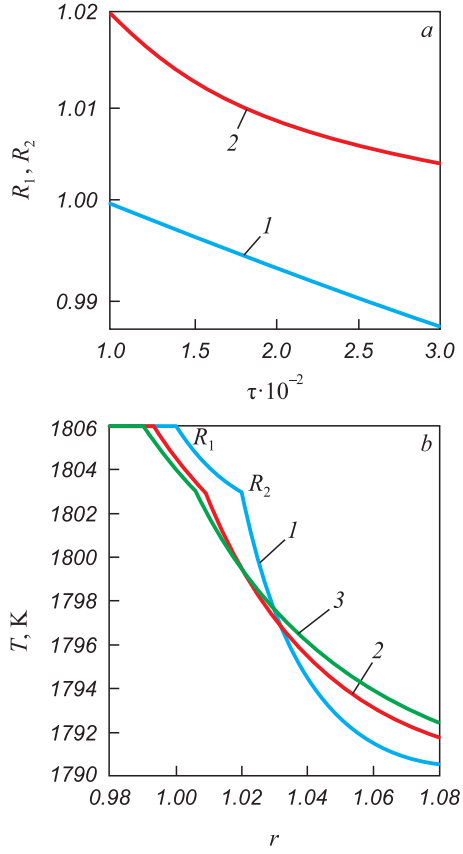

Fig. 4. Calculation results for T_{w1} = 1811 K, T^* = 1806 K, T^{**} = 1803 K, T_0 = 1790 K, R_0 = 1 μm: *a* – dependences of the radial coordinates of the crystallization front on time (*1* – boundary of transition between phases *1* and *2*; *2* – boundary of transition between phases *2* and *3*); *b* – temperature dependences on the coordinate at different time (*1* – τ = 0.01; *2* – τ = 0.02; *3* – τ = 0.025)

Рис. 4. Результаты вычислений при T_{w1} = 1811 K, T^* = 1806 K, T^{**} = 1803 K, T_0 = 1790 K, R_0 = 1 мкм: *a* – зависимости радиальных координат фронта кристаллизации от времени (*1* – граница перехода между фазами *1* и *2*; *2* – граница перехода между фазами *2* и *3*); *b* – зависимости температуры от координаты в различные моменты времени (*1* – τ = 0,01; *2* – τ = 0,02; *3* – τ = 0,025)

References / Список литературы

1. Sosnin N.A., Ermakov S.A., Topolyanskii P.A. *Plasma Technologies. A Guide for Engineers*. SPb.: izd. Politekhnicheskogo un-ta; 2013;406. (In Russ.).
Соснин Н.А., Ермаков С.А., Тополянский П.А. *Плазменные технологии. Руководство для инженеров*. СПб.: изд. Политехнического ун-та; 2013;406.
2. Damon J., Schüßler P., Mühl F., Dietrich S., Schulze V. Short-time induction heat treatment of high speed steel AISI M2: Laboratory proof of concept and application-related component tests. *Materials & Design*. 2023;230:111991. https://doi.org/10.1016/j.matdes.2023.111991
3. Park G.-W., Shin S., Kim J.-Y., Koo Y.-M., Lee W., Lee K.-A., Park S.S., Jeon J.B. Analysis of solidification microstructure and cracking mechanism of a matrix high-speed steel deposited using directed-energy deposition. *Journal of Alloys and Compounds*. 2022;907:164523. https://doi.org/10.1016/j.jallcom.2022.164523
4. Malushin N.N., Romanov D.A., Kovalev A.P., Osetkovskii V.L., Bashchenko L.P. Structural-phase state of a heat-resistant alloy of high hardness formed by plasma surfacing in nitrogen medium and high-temperature tempering. *Izvestiya*

vuzov. Fizika. 2019;62(10(742)):106–111. (In Russ.).
https://doi.org/10.17223/00213411/62/10/106

Малушин Н.Н., Романов Д.А., Ковалев А.П., Осетковский В.Л., Бащенко Л.П. Структурно-фазовое состояние теплостойкого сплава высокой твердости, сформированного плазменной наплавкой в среде азота и высокотемпературным отпуском. *Известия вузов. Физика*. 2019;62(10(742)):106–111.
https://doi.org/10.17223/00213411/62/10/106

5. Aleksandrov D.V., Aleksandrova I.V., Ivanov A.A., Malygin A.P., Nizovtseva I.G. Nonlinear analysis of the stability of solidification with a mushy zone. *Russian Metallurgy (Metally)*. 2014;2014(8):606–617.
https://doi.org/10.1134/S0036029514080035

Александров Д.В., Александрова И.В., Иванов А.А., Малыгин А.П., Низовцева И.Г. Нелинейный анализ устойчивости затвердевания с областью фазового перехода. *Расплавы*. 2014;(2)27–40.

6. Aleksandrov D.V., Aleksandrova I.V., Ivanov A.A., Starodumov I.O., Toropova L.V. Directional solidification with a two-phase zone taking into account the dependence of liquid phase density on temperature and impurity concentration. *Rasplavy*. 2020;(1):37–45. (In Russ.).
https://doi.org/10.31857/S0235010620010028

Александров Д.В., Александрова И.В., Иванов А.А., Стародумов И.О., Торопова Л.В. Направленное затвердевание с двухфазной зоной с учетом зависимости плотности жидкой фазы от температуры и концентрации примеси. *Расплавы*. 2020;(1):37–45.
https://doi.org/10.31857/S0235010620010028

7. Alexandrov D.V., Toropova L.V. The role of incoming flow on crystallization of undercooled liquids with a two-phase layer. *Scientific Reports*. 2022;12:17857.
https://doi.org/10.1038/s41598-022-22786-w

8. Worster M.G. Natural convection in a mushy layer. *Journal of Fluid Mechanics*. 1991;224:335–359.
https://doi.org/10.1017/S0022112091001787

9. Lahiri A., Choudhury A. Theoretical and numerical investigation of diffusive instabilities in multicomponent alloys. *Journal of Crystal Growth*. 2017;459:1–12.
http://dx.doi.org/10.1016/j.jcrysgro.2016.11.046

10. Sekerka R.F. Morphological stability. *Journal of Crystal Growth*. 1968;3-4:71–81.
https://doi.org/10.1016/0022-0248(68)90102-4

11. Alexandrov D.V. Solidification with a quasiequilibrium mushy region: exact analytical solution of nonlinear model. *Journal of Crystal Growth*. 2001;222(4):816–821.
https://doi.org/10.1016/S0022-0248(00)00960-X

12. Elsaid A., Helal S.M. Moving Taylor series for solving one-dimensional one-phase Stefan problem. *Alexandria Engineering Journal*. 2022;61(9):7121–7128.
https://doi.org/10.1016/j.aej.2021.12.055

13. Lykov A.V. *Theory of Thermal Conductivity*. Moscow: Vysshaya shkola; 1967;599. (In Russ.).

Лыков А.В. *Теория теплопроводности*. Москва: Высшая школа; 1967;599.

14. Sergeev S.A. Mathematical modeling of unsteady thermal conductivity of spherical particle crystallization in a melt with moving boundaries. *Issledovano v Rossii*. 2003;(6):664–672.

Сергеев С.А. Математическое моделирование нестационарной теплопроводности кристаллизации частицы сферической формы в расплаве с движущимися границами. *Исследовано в России*. 2003;6:664–672.

15. Chen M.W., Wang Z.D. The evolution and morphological stability of a particle in a binary alloy melt. *Journal of Crystal Growth*. 2023;607:127113.
https://doi.org/10.1016/j.jcrysgro.2023.127113

16. Formalev V.F., Rabinskii L.N. On a Stefan-type problem with two unsteadily moving boundaries of phase transformations. *Izvestiya RAN. Energetika*. 2014;(4):74–81. (In Russ.).

Формалев В.Ф., Рабинский Л.Н. О задаче типа Стефана с двумя нестационарно подвижными границами фазовых превращений. *Известия РАН. Энергетика*. 2014;(4):74–81.

17. Kartashov E.M. Analytical methods for solving boundary value problems of unsteady thermal conductivity in regions with moving boundaries. *Engineering and Physics Journal*. 2001;74(2):171–195.

Карташов Э.М. Аналитические методы решения краевых задач нестационарной теплопроводности в областях с движущимися границами. *Инженерно-физический журнал*. 2001;74(2):171–195.

18. Carslaw H.S., Jaeger J.C. *Conduction of Heat in Solids*. London: Oxford University Press; 1947.

Карслоу Г., Егер Д. *Теплопроводность твердых тел*. Москва: Наука; 1964;488.

19. Lyakishev N.P. *State Diagrams of Double Metal Systems*. In 3 vols. Vol. 2. Moscow: Mashinostroenie; 1997;1024. (In Russ.).

Лякишев Н.П. *Диаграммы состояния двойных металлических систем*. В 3 т. Т. 2. Москва: Машиностроение; 1997;1024.

20. Chen M.-W., Wang Y., Guo H. The effect of anisotropic surface tension on interfacial evolution of a particle in the binary alloy melt. *Journal of Crystal Growth*. 2019;510:32–39.
https://doi.org/10.1016/j.jcrysgro.2018.12.032

Information about the Authors | Сведения об авторах

Sergei A. Nevskii, *Dr. Sci. (Eng.), Assist. Prof. of the Chair of Natural Sciences named after Professor V.M. Finkel,* Siberian State Industrial University
ORCID: 0000-0001-7032-9029
E-mail: nevskiy_sa@physics.sibsiu.ru

Lyudmila P. Bashchenko, *Cand. Sci. (Eng.), Assist. Prof. of the Chair "Thermal Power and Ecology",* Siberian State Industrial University
ORCID: 0000-0003-1878-909X
E-mail: luda.baschenko@gmail.com

Сергей Андреевич Невский, *д.т.н., доцент кафедры естественнонаучных дисциплин им. профессора В.М. Финкеля,* Сибирский государственный индустриальный университет
ORCID: 0000-0001-7032-9029
E-mail: nevskiy_sa@physics.sibsiu.ru

Людмила Петровна Бащенко, *к.т.н., доцент кафедры теплоэнергетики и экологии,* Сибирский государственный индустриальный университет
ORCID: 0000-0003-1878-909X
E-mail: luda.baschenko@gmail.com

Oleg A. Peregudov, *Cand. Sci. (Eng.), Vice-Rector for Youth Policy and Educational Activities,* Omsk State Technical University
ORCID: 0000-0001-5154-5498
E-mail: Olegomgtu@mail.ru

Олег Александрович Перегудов, *к.т.н., проректор по молодежной политике и воспитательной деятельности,* Омский государственный технический университет
ORCID: 0000-0001-5154-5498
E-mail: Olegomgtu@mail.ru

Contribution of the Authors / Вклад авторов

S. A. Nevskii – statement of the problem, development of a model of the section boundaries movement, discussion of the results.
L. P. Bashchenko – calculations, discussion of the results, design of the article.
O. A. Peregudov – discussion of the results, analysis of literary sources on the Stefan problem.

С. А. Невский – постановка задачи, разработка модели движения границ раздела, обсуждение результатов.
Л. П. Бащенко – проведение расчетов, обсуждение результатов, оформление статьи.
О. А. Перегудов – обсуждение результатов, анализ литературных источников по задаче Стефана.

Received 19.06.2023
Revised 27.06.2023
Accepted 28.06.2023

Поступила в редакцию 19.06.2023
После доработки 27.06.2023
Принята к публикации 28.06.2023